

Multi-Wavelength digital holographic metrology

Carl C. Aleksoff

Coherix, Inc., 3980 Ranchero Drive, Ann Arbor, MI 48108

ABSTRACT

A digital holographic metrology technique is described for measuring the three-dimensional shape of manufactured parts. The technique uses optical fibers to set up a near equal path interferometer, steps through multiple frequencies with a tunable laser, steps through multiple phases using a fiber based phase shifter, uses an off-axis parabolic mirror to collimate the light, and generates a digital hologram that leads to surface flatness measurements accuracies better than 1 micron over large surfaces. An example result for an automobile engine part is given using a Coherix Inc., Shapix™ 2000 instrument.

Keywords: Holography, interferometry, metrology, flatness, 3D shapes

1. INTRODUCTION

One of the most useful outgrowths of Emmett Leith's holographic work is its use in metrology¹. The measurement of parts via holographic techniques started early at the Willow Run Labs of the University of Michigan with object deformation interferometry^{2, 3}, shape contouring⁴, and vibration analysis^{5, 6}. In this paper we will consider a more modern outgrowth of using multi-wavelength digital holography to generate 3D (three dimensional) computer-based precision imagery of manufactured parts. These digital holographic techniques have been incorporated into the Coherix Shapix™ systems*, for which Emmett Leith was a consultant.

The output digital image is a 2D array of numbers, where each number represents a height H from a reference plane for a pixel. This data can be processed to generate various views on a monitor or mined for features such a deviation from specified shape or surface roughness.

The basic multi-wavelength measurement concept can be described from the standpoint of synthetic-aperture laser-radars^{7, 8} or via interferometers⁹. In this paper will develop the basics of the process from an interferometric perspective because we are describing an image plane holographic system where each acquired image pixel can be described as part of a simple interferometer.

2. THEORY

Consider Fig. 1, which schematically illustrates the surface measuring (SM) system under consideration. A frequency tunable laser is used as the light source. The laser output feeds a polarization maintaining single mode fiber. A variable coupler divides the laser light into two fibers. The light in one fiber illuminates the object via a parabolic mirror that collimates the light wave. The reflected light from the object is then viewed with a camera via the parabola and a cube beamsplitter. The camera lens images the object onto the camera detector array. The second fiber generates the reference wave that is aligned via the beamsplitter with the object wave. The reference source has the same apparent lateral position and distance as the convergence point of the light from the object. The reference fiber includes a variable phase shifter that allows the phase of the reference light to be shifted with respect to the phase of the object light.

Consider a single detector in the camera of width size Δx by Δy , which corresponds to a size $\Delta X = M \Delta x$ and $\Delta Y = M \Delta y$ on the object, where M is the magnification for the SM system. If the laser light is linearly polarized and the amplitude is described by the signal $A \exp(-i2\pi\nu t)$ where ν is the frequency of the light, then pixel output from the camera is proportional to

$$I = \left| A_{obj} \exp[-i2\pi\nu(t - \tau_{obj})] + A_{ref} \exp[-i2\pi\nu(t - \tau_{ref}) + i\phi] \right|^2 \quad (1)$$

where τ_{obj} and τ_{ref} are the time delays of the light from the laser to the detector for the object arm and the reference arm, respectively, and ϕ is the phase shift imparted by the fiber phase shifter. This expression can be reduced to

$$I = |A_{obj}|^2 + |A_{ref}|^2 + 2|A_{obj}A_{ref}|\cos[2\pi\nu(\tau_{obj} - \tau_{ref}) - \phi] \quad (2)$$

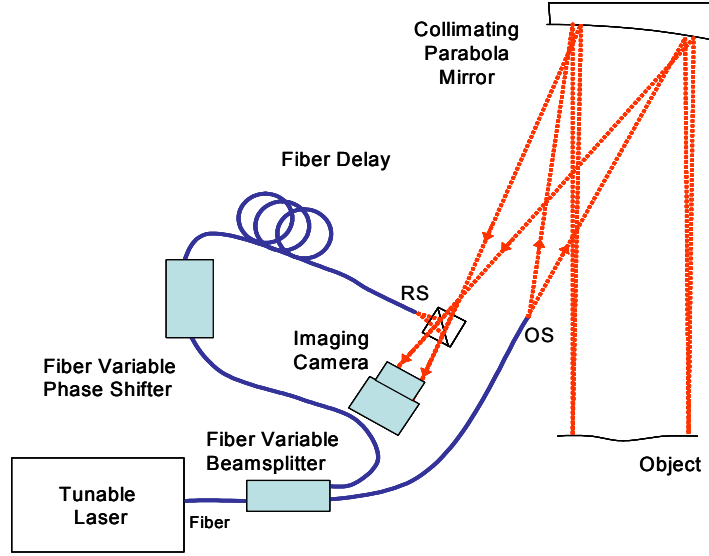


Fig. 1 The optical arrangement is shown for measuring the object height as a function lateral position. The illumination source (OS) is the end of one fiber and the reference source (RS) is at the other end. The reference source is at the same apparent position and distance from the camera as the focus of light via the parabola from the object. The camera images the object as well as accepting a coaxial reference wave for interference via the cube beamsplitter.

Now we can write that

$$2\pi\nu(\tau_{obj} - \tau_{ref}) = \frac{2\pi}{\lambda}(OPL_{obj} - OPL_{ref}) = \frac{4\pi H}{\lambda} \quad (3)$$

where λ is the free space wavelength associated with the frequency ν , OPL_{obj} and OPL_{ref} are the optical path lengths through the indicated arms that accounts for the effective refractive index of the fiber, and H is the height measured from the matched path length position. The length of the fiber in the reference arm is chosen to produce a convenient reference plane for the height measurements.

Thus, the basic interferometric equation for the detected signal is

$$I(\phi) = |A_{obj}|^2 + |A_{ref}|^2 + 2|A_{obj}A_{ref}|\cos\left[\frac{4\pi H}{\lambda} - \phi\right] \quad (4)$$

A number of different phase shifting techniques can be used to extract the height information. The technique of choice depends on the noise sources to be mitigated¹⁰. Here, for illustrative purposes we note that if we change the reference phase by $\pi/4$ increments we can form the following expression from four measurements.

$$\Theta(\lambda) = \arctan\left[\frac{I(\pi/4) - I(3\pi/4)}{I(0) - I(\pi/2)}\right] = \frac{4\pi H}{\lambda} - \text{mod}(2\pi) \quad (5)$$

or that

$$H = \frac{\lambda}{4\pi} [\Theta(\lambda) + \text{mod}(2\pi)] = \frac{\lambda\Theta(\lambda)}{4\pi} + n \frac{\lambda}{2} \quad (6)$$

Thus, these four measurements give us the height as the fraction of the wavelength but within some unknown integer multiple n of half wavelengths. In order to determine integer n we can use multiple wavelengths and Fourier analysis.

If we recognize that the modulus term can be taken into account by using the periodicity of a sinusoid and that the measured phase corresponds to starting phase, then simply adding the sinusoids together will give a peak signal at the height of the surface. That is, we form following summation and look for the peak

$$\frac{1}{K} \sum_{k=1}^K \cos \left[4\pi \frac{h}{\lambda_k} - \Theta(\lambda_k) \right] \quad (7)$$

where K gives the number of different optical frequencies used. Notice that we use only unity valued cosines which implies we are using the measured phase information only to find the height. Now one issue is that the actual position of peak using the sum of cosines is system phase dependent. If we use complex notation, and take the magnitude, then the highly oscillating term is removed and only the envelope remains. The envelope peak is phase independent. Thus, we use

$$S(h) = \left| \frac{1}{K} \sum_{k=1}^K \exp \left[4\pi \frac{h}{\lambda_k} - \Theta(\lambda_k) \right] \right| \quad (8)$$

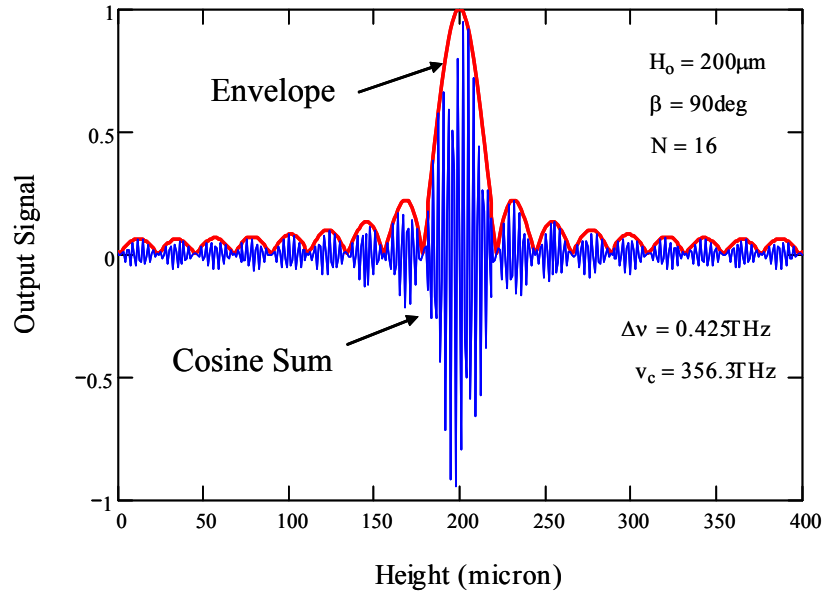


Fig. 2. This figure simulates the output between summation of cosines and the envelope (magnitude of the complex representation). The surface height was 200 microns. The results are for N frequencies with spacing of $\Delta\nu$ and carrier frequency ν_c .

This is illustrated in Fig. 2 for 16 different frequencies equally spaced by 425GHz at a carrier frequency of 356 THz (which nominally corresponds to 1 nm spacing centered at a wavelength of 840 nm) where the surface is 200 mm above the reference.

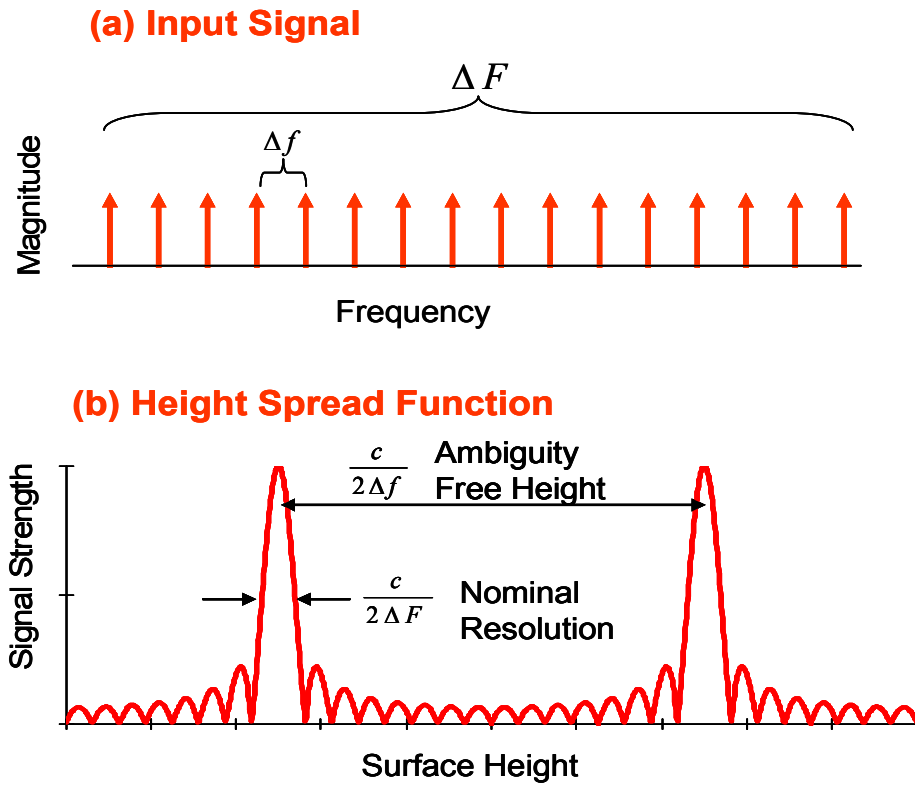


Fig. 3. These diagrams show the basic relationships the input and output data. The input data is a set of delta functions with the frequency spacing of the measurement frequencies (assumed equal spacing) and measured phases. The output is the magnitude of the Fourier Transform of the input data. The calculated surface height is at the first peak of the output.

Realizing that we have established a Fourier Transform (FT) technique for finding the height, we can use the FT properties to understand the properties of using such a technique. These are illustrated in Fig. 3. We start with the normalized input laser frequencies as a set of delta functions and assign the measured phase to each frequency. Here we take 16 equally spaced frequencies. The absolute frequencies are not necessary, only the relative spacing Δf and the frequency band ΔF . The magnitude of the FT of the input gives a peak of width $c/2\Delta F$ at the height of the surface. However, due to discrete nature of the input, the output has periodic peaks at spacing of $c/2\Delta f$, which is known as the ambiguous free height range. This ambiguous free height range limits the range we can make height measurements without encountering extra peaks. The finer the frequency spacing, the greater the ambiguous free height range, and the greater the bandwidth, the finer the resolution.

Other combinations of laser frequencies, rather than equally spaced, such as non-redundant spaced frequencies and other weighting of the amplitudes, such as Hamming can be used to alleviate the ambiguity-free-range or improve sidelobe levels as might be required to improve the measurements, given certain noises.

Now under the assumption that only a single surface height exists over the pixel being measured (i.e., no significant surface roughness), then we can super-resolve by determining the peak position to a much greater accuracy than the nominal width of the peak gives. The resolution to which the peak position (i.e., surface height) can be determined is proportional to $c/(2\Delta F\sqrt{SNR})$, where SNR is the signal-to-noise ratio for the measurements. In practice, the super-resolution improvement is a factor of 10 to 100.

The electronically controlled variable splitter is used to guarantee that the maximum SNR is obtained. The splitter is set so that the modulation depth of the interferometer fringes is maximized which also maximizes the SNR.

3. SYSTEM RESULTS

In this section we will show results in measuring the flatness of engine block deck. It is important for sealing purposes that the deck be flat at critical areas. A Shapix system configured to accept engine blocks is shown in Fig. 4. A close up picture of an engine block is shown in Fig. 5. Resulting measurement are shown in Fig. 6a and 6b for one deck side that encompasses 5 cylinders. This flatness image is a stitched image of three subsets of overlapping data with each subset of data covering up to about 12 inches square and encompassing up to four megapixels. The height variation can be seen in the perspective display of the deck. In Figure 6a the deck cutting tool was new. In Figure 6b the result was obtained after the cutting tool had cut 1800 decks. The deterioration of the flatness of the deck is clearly evident. In a production setting, the rapid generation of a 3D image, would allow the manufacturing process to be adjusted early to remedy a developing deterioration before it become serious.

A line of height measurements near one long edge is shown in Fig. 7 This plot shows two overlapping sets of height measurements, one made with the Coherix Shapix 2000 and the other made with a Zeiss Prismo CMM (Coordinate Measuring Machine), showing excellent agreement

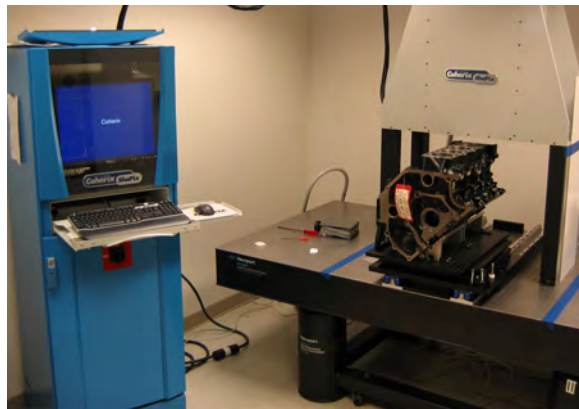


Fig.4. The Shapix system with an engine block inserted for measurement.

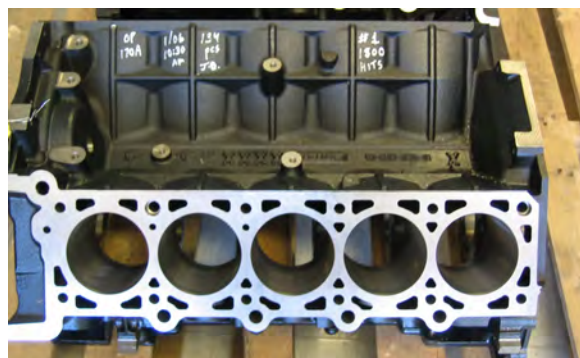


Fig. 5. A picture of the engine showing the cylinder deck face to be measured for flatness

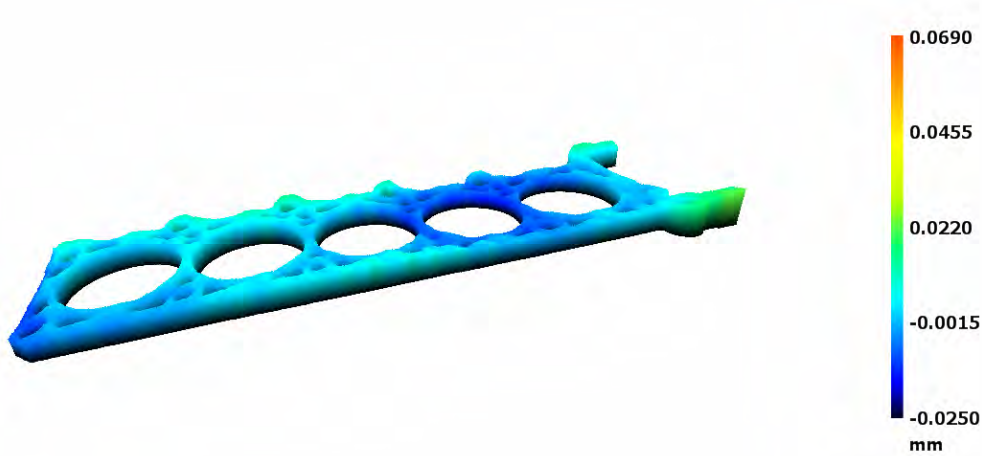


Fig. 6a A Shapix measured engine cylinder deck is shown as a 3D perspective image. This deck was cut with a new tool bit.

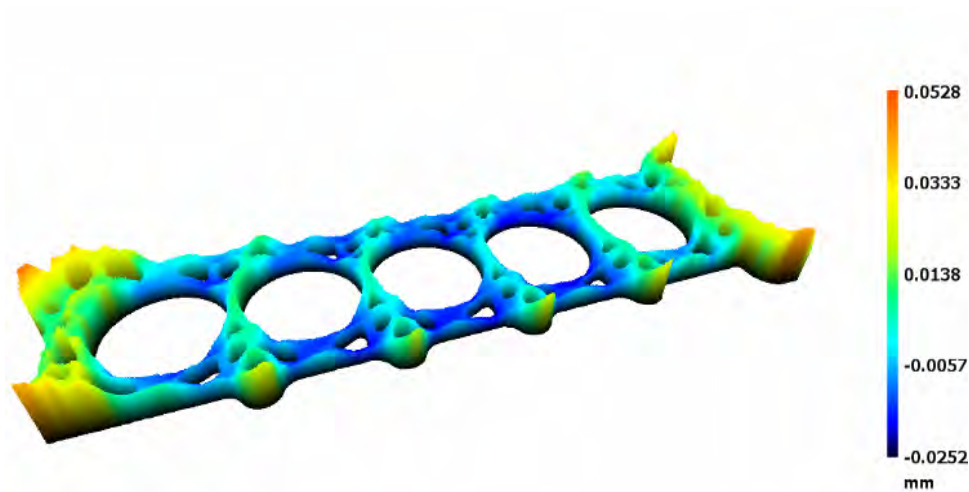


Fig. 6b. A Shapix measured engine cylinder deck is shown as a 3D perspective image. This deck was the 1800 unit cut with the tool bit.

CONCLUSIONS

We have presented some theoretical foundations for 3D digital-holographic imaging using multiple wavelength and interferometric principles. Practical measurement results were presented for an engine cylinder deck. The optical measurements were shown to correlate very accurately with mechanical measurements.

The development of the Coherix Shapix system has taken many years and many people. We would like to acknowledge the more recent development contributions of Ron Swonger, Alex Klooster, Mike Mater, and Greg Dale that have made the reported fine 3D measurements possible.

*The Shapix technology is protected by multiple U. S. and foreign patents and patents pending.

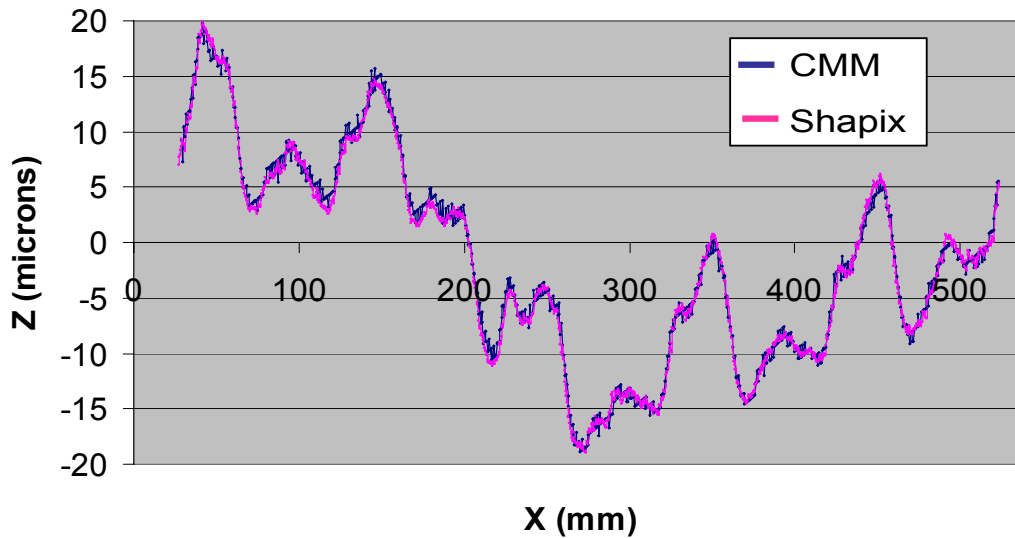


Fig. 7. This plot shows two measurements of the height near one edge of the engine head shown in Fig. 6b. One measurement is with a CMM and the other with the Shapix system, showing excellent agreement.

REFERENCES

1. E. N. Leith and J. Upatnieks, "Wavefront Reconstruction with Diffused Illumination and Three-Dimensional Objects," *J. Opt. Soc. Amer.* **54**, 1295 (1964).
2. K. A. Haines and B. P. Hildebrand, "Interferometric Measurements on Diffuse Surfaces by Holographic Techniques," *IEEE Trans. Instrum. Meas.* **IM-15**, 149 (1966).
3. A. A. Friesem and C. M. Vest, "Detection of Micro-Fractures by Holographic Interferometry," *Appl. Opt.* **8**, 1253 (1969).
4. J. S. Zelenka and J. R. Varner, "A New Method for Generating Depth Contours Holographically," *Appl. Opt.* **7**, 2107 (1968).
5. K. A. Stetson and R. L. Powell, "Interferometric Vibration Analysis by Wavefront Reconstruction," *J. Opt. Soc. Amer.* **55**, 1593 (1965).
6. C. C. Aleksoff, "Temporally Modulated Holography," *Appl. Opt.* **10**, 1329 (1971).
7. J. C. Marron and K. S. Schroeder, "Three-dimensional lensless imaging using laser frequency diversity," *Appl. Opt.* **31**, 255 (1992).
8. C. C. Aleksoff, "Optical Range-Doppler Imaging," *The Infrared and Electro-Optical Systems Handbook*, Editors J. S. Accetta and D. L. Shumaker, SPIE Press, Vol. 8, 110 (1993).
9. J. C. Marron and K. W. Gleichman, "Three-dimensional imaging using a tunable laser source," *Opt. Eng.* **39**(1), 47 (Jan. 2000)
10. K. J. Gasvik, *Optical Metrology*, 3rd Edition, Chap. 11, John Wiley & Sons, (2002)